TENTH AUSTRALASIAN FLUID MECHANICS
CONFERENCE - UNIVERSITY OF MELBOURNE
11-15 DECEMBER 1989

A NUMERICAL STUDY OF TURBULENT FLOW IN A CHANNEL WITH A WAVY WALL

Juliet T. CHON and V.C. PATEL

Department of Mechanical Engineering
and Iowa Institute of Hydraulic Research
The University of Iowa
Iowa City, Iowa 52242
USA

ABSTRACT

A numerical method for the solution of the Reynolds-averaged Navier-Stokes equations, together with a two-layer turbulence model, has been used to study the turbulent flow in a two-dimensional channel with a wavy wall. Comparisons of calculations with experiments demonstrate the effects of alternating curvatures and pressure gradients, and multiple separations and reattachments. The numerical method and the turbulence model capture the overall features of such a flow.

INTRODUCTION

The study of flow over a wavy boundary is of interest in a number of physical phenomena. Examples include generation of water waves by wind, evolution of sand dunes in deserts and sediment dunes in rivers, and melting of ice covers on rivers. Flow past wavy walls is also of interest in the enhancement of heat and mass transfer, and possibly drag reduction. From the perspective of viscous-flow theory, the flow over a wavy boundary, whether laminar or turbulent, is much more complex than that over a flat surface because of the additional parameters and flow phenomena that are involved. For example, for fully-developed flow in a channel or pipe, we have, in addition to the Reynolds number, the ratios λ/h and a/λ , where a is wave amplitude, λ is the wave length, and h the channel half-height or pipe diameter. For developing boundary-layer flows, the conditions of the boundary layer upstream and the number of waves must be considered. In either case, for wave amplitudes greater than some critical value at any Reynolds number, the flow involves multiple regions of separation and reattachment. Description of turbulent flow past a wavy surface involves a number of challenges. In addition to the effects of the alternating favorable and adverse pressure gradients, and convex and concave surface curvatures on the turbulence, there is the difficulty of predicting the separation and reattachment points. For laminar as well as turbulent flows, there exists the possibility of self-induced unsteadiness of the flow in the cavities and associated vortex shedding.

For the various reasons noted above, a numerical method has been developed for the solution of the Navier-Stokes equations for laminar flow, and the Reynolds-averaged Navier-Stokes equations for turbulent flow along a wavy surface of arbitrary shape. The present paper is concerned with the application of this method to turbulent flow in a two-dimensional channel, one wall of which is sinusoidally wavy and the other is flat. This configuration was selected because it has been studied rather extensively over a number of years in a series of experiments conducted by Hanratty and his students (see Table 1).

NUMERICAL METHOD AND EXPERIMENTAL INFORMATION

The numerical method used here solves the Reynolds equations for unsteady flow in generalized, nonorthogonal, numerically generated coordinates. No a priori simplifications or approximations are made in the equations. The two-layer approach to turbulence modelling suggested by Chen and Patel (1988) has been used to test its suitability in the present flow. In this approach, the standard two-equation k-ε turbulence model is combined with a simpler, one-equation model for the flow close to the wall. The momentum and turbulence transport equations are discretized using analytic solutions of the linearized equations, and the pressure-velocity coupling is made through the continuity equation using the SIMPLER algorithm. Details of the method and applications to different configurations with laminar and turbulent flows are given in Richmond (1987) and Tyndall (1988).

The experiments of Hanratty et al. were all conducted in the same water-channel facility, although there were variations in the measurement techniques. In a rectangular channel 2 in. high, 24 in. wide, and 35 ft. long, removable wavy surfaces were placed in the last 27 inches of the bottom wall. In all cases, a wave length of 2 in. was used, with ten waves in the test section. The waves were sinusoidal, so that the surface height y_S was defined by $y_S = a \sin \alpha x$, where $\alpha = 2\pi/\lambda$ is the wave number. Fully-developed flow was obtained in the channel before the test section, and in all cases spatially periodic conditions were found to have been established early in the wavy test section. Therefore, most detailed measurements were made only over a single wave.

Table 1 summarizes the measurements made and the parameters used in the various experiments, including the ratio $2a/\lambda$. and the Reynolds number, $Re = Uh/\nu$, based on the bulk velocity U, channel half-height h, and the kinematic viscosity ν. Note that $2h/\lambda = 1$ in all the experiments. Table 1 also notes the most important flow characteristics observed in the experiments. Depending upon the Reynolds number and wave amplitude, different flow regimes are possible.

CALCULATIONS AND RESULTS

Two sets of calculations, corresponding to an experiment of Frederick (1986) in the linear response regime, and one of Kuzan (1986) in the nonlinear separated-flow regime, have been performed. These cases are identified in Table 1. Each calculation was performed in two parts, one for the upstream straight channel to establish the proper initial conditions and the other for a portion of the straight and the wavy sections.

For the straight portion, a length of 80 channel widths was used and calculations were made with 81 streamwise and 99 cross-stream nodes, with the first grid point off the walls at $y^+ \sim 0.01$. Starting with approximate initial conditions, converged solutions were obtained in about 100 iteratiions (or time steps). The velocity field and turbulence parameters calculated in the fully-developed flow at the downstream end were then used as the initial conditions for the subsequent wavy-wall calculations. The same distribution of grid across the channel was maintained in both calculations so that the initial conditions could be used without interpolation. It should be emphasized that this method of establishing initial conditions requires only the specification of the channel Reynolds number, all other information being generated consistently from the solution of the governing equations. This removes the usual uncertainties about initial conditions and makes the present calculations truly predictive.

In the presentation of the results, all quantities, including pressure and friction coefficients, are normalized by the bulk velocity in the channel, the wave length, and the fluid properties.

Wavy wall, $2a/\lambda = 0.03125$, $Re = 12{,}800$: attached flow

The solution domain shown in Figure 1(a) was covered with 328 x 99 grid points. Over each of the six sinusoidal waves in the lower boundary, there are 50 nodes. An upstream section, 4λ in length, allows the flow to adjust to the wavy section, and a downstream section, of length λ, is used for flow recovery. The initial conditions were applied at $x = 0$. The wavy section begins with a positive slope to match the experimental configuration.

Six hundred iterations were used, taking approximately 60 minutes on a Cray XMP-48. As the pressure and friction coefficients plotted in Figures 1(b) and (c) show, satisfactory convergence was achieved in fewer than 450 iterations. It is also seen that there is a pressure drop along the channel, superimposed on the changes in pressure over the boundary waves. Initially the pressure and friction coefficients on both the upper and lower boundaries coincide, as would be expected in a duct with flat walls. The influence of the wavy section is seen to begin upstream of its origin, which is at $x = 4.0$. Conditions at the upper boundary appear to be little affected by the wavy section. The behaviour of both the pressure and the friction coefficients in the straight exit section imply that this section was not long enough to allow for proper recovery of the flow to straight-duct conditions.

Figures 1(b) and (c) indicate that the flow becomes spatially periodic rather quickly, establishing almost fully periodic conditions by the second or third wave. Figure 2 shows the axial velocity profiles at stations one-fifth of a wave length (72 deg) apart, beginning with the peak of the fifth wave at $x = 8.25$ and ending with the peak of the sixth at $x = 9.25$. Both linear and semi-logarithmic plots are shown. The data are those of Frederick (1986), gathered over the eighth of ten waves. The profiles are shown only to a height $n = 0.5$, n being the distance along the grid line originating from the wavy wall at the appropriate x station. The difference between this and the normal distance is insignificant. The first and last stations, labelled $\phi = 0$ and 360 deg, respectively, correspond to the wave crests.

From the linear plots in Figure 2 it is seen that the measured velocities are larger than the calculated ones for n greater than about 0.2. Because the duct used in the experiments had an aspect ratio (channel width to mean-depth ratio) of only 12, with an approach section 70 hydraulic diameters long and a test section 29 wavelengths long, end-wall effects are most likely being observed in these higher core velocities. Hence, the experiments presumably do not represent truly two-dimensional flow. Closer to the wall, but still outside the law-of-the-wall region, the agreement of the calculated and experimental results is good until about the trough of the wave, and thereafter the velocities are slightly overpredicted.

The semi-logarithmic plots in Figure 2 were made using the calculated and measured friction velocities. Also shown for comparison by the dashed line is the standard logarithmic law, $u^+ = \kappa^{-1} \ln y^+ + B$, with $\kappa = 0.418$ and $B = 5.5$. The standard law is clearly not applicable in regions of strong adverse and favorable pressure gradients. The calculated profiles follow the experimental trends rather well but do not completely match the data. Initially, at $\phi = 0$ deg, the pressure gradient is mildly favorable (see Figure 3) and the velocity distribution lies below the logarithmic law. By the next station, $\phi = 72$ deg, the pressure gradient is adverse and the profile lies above the logarithmic law. At the following station, $\phi = 144$ deg, the adverse gradient is strong and the friction velocity is near its minimum. Here, we observe the greatest departures from the logarithmic law as well as the greatest disagreement between the calculated and experimental values. However, the trend is well predicted. As the peak in the adverse pressure gradient is passed, the velocity profile begins to shift back towards the logarithmic law, until $\phi = 216$ deg, where agreement is reestablished due to near zero pressure gradient at this location. At the next two stations, $\phi = 288$ and 360 deg, the favorable pressure gradient causes departures of the velocity profiles below the logarithmic law, which the calculations predict faithfully. Note that the solution at the last station was found to be in excellent agreement with that at the first, confirming the spatial periodicity of the flow. Finnicum and Hanratty (1988) have recently examined the velocity distributions in favorable pressure gradients and the possibilities of local relaminarization.

The pressure and friction coefficients along a wave, and the wave profile, are shown in Figure 3. Both quantities show a phase shift with respect to the surface. The pressure lags the suface profile by about 200 deg whereas the friction anticipates it by almost 45 deg. The agreement between the calculated and measured values of the friction coefficient is good except in the region $8.50 < x < 9.34$, where the predicted values are larger.

Wavy wall, $2a/\lambda = 0.20$, $Re = 8{,}160$: separated flow

The calculations for this extreme case were carried out with the solution domain and grid numbers similar to those used in the first case, except that the upstream and downstream straight sections were 3λ and 2λ, respectively. This change allowed a longer downstream recovery length. Figure 4 shows the pressure and friction coefficients. Again the results on the upper and lower walls are in agreement initially, but in this case the solution on the upper wall appears to vary more from a standard straight-duct behavior than in the previous case shown in Figure 1 Recovery in the downstream section is more closely achieved. However, it is clear that a much longer section is required to reestablish straight-channel conditions.

Comparison of Figures 1 and 4 clearly indicate the additional complexities of the second case. Harmonic analysis of the two sets of results would confirm the classification of Hanratty et al., that the former shows nearly linear response while the latter is highly nonlinear. The calculations for the present case of $2a/\lambda = 0.20$ indicate flow separation not only in the waves but also ahead of the first wave. The distributions of pressure and friction coefficients, and the calculated streamlines over the fifth wave are shown in Figure 5. Separation is predicted at $x = 7.33$ and reattachment at $x = 7.98$. Measuring from the top of the upstream crest ($x = 7.25$), these points are located at Δx of 0.08 and 0.73 , respectively. Kuzan (1986) measured a separation point at $\Delta x = 0.12$, with reattachment at $\Delta x = 0.77$. For the same configuration but a different Reynolds number, Buckles et al. (1984) measured separation at $\Delta x = 0.14$ and reattachment at $\Delta x = 0.69$. Thus, the predicted positions are in fairly good agreement with data.

CONCLUDING REMARKS

Limitations of space have precluded the presentation and discussion of many other interesting aspects of the flow over wavy walls. For example, we have not examined some important details of the solutions, such as velocity profiles in separated flow, and distributions of the various turbulence parameters which are explicitly calculated with the present model. From the limited results presented here, however, it is clear that the numerical method is quite successful in calculating flows with multiple separations and reattachments with a reasonable amount of computer time, and the two-layer turbulence model of Chen and Patel (1988) appears to capture most of important physical features of such flows. The results also demonstate the breakdown of the standard law of the wall in strong pressure gradients.

The flow in a channel with a wavy wall is obviously a challenging test case for numerical methods and turbulence models. The overall numerical approach described here is general enough to begin a more in-depth study of the physics of flows over wavy walls of arbitrary shape and extend it to consider the many practical flow phenomena which involve wavy boundaries.

ACKNOWLEDGEMENTS

This research was partially supported by the Office of Naval Research, under Contract N00014-88-K-0001. The calculations were performed on the CRAY XMP/48 of the NCSA, Champaign, Illinois.

REFERENCES

Abrams, J. (1984), Ph.D. Thesis, Dept. Chem. Engr., Uni. Illinois, Urbana, IL.

Abrams, J. and Hanratty, T.J. (1985), J. Fluid Mech., v. 151, pp. 443-455.

Buckles, J., Hanratty, T.J. and Adrian, R.J. (1984), J. Fluid Mech., v. 140, pp. 27-44.

Chen, H.C. and Patel, V.C. (1988), AIAA J., v. 26, pp. 641-648.

Finnicum, D.S. and Hanratty, T.J. (1988), A.I.Ch.E. Journal, v. 34, pp. 529-540.

Frederick, K.A. (1986), Ph.D. Thesis, Dept. Chem. Engr., Uni. Illinois, Urbana, IL.

Frederick, K.A. and Hanratty, T.J. (1986), Expts. in Fluids, v. 6, pp. 477-486.

Kuzan, J.D. (1986), Ph.D. Thesis, Dept. Chem. Engr., Uni. Illinois, Urbana, IL.

Richmond, M.C. (1987), Ph.D. Thesis, Dept. Mech. Engr., Uni. Iowa, Iowa City, IA.

Thorsness, C.B., Morrisroe, P.E. and Hanratty, T.J. (1978), Chem. Eng. Sci., v. 33, pp. 579-592.

Tyndall, J. (1988), M.S. Thesis, Dept. Mech. Engr., Uni. Iowa, Iowa City, IA.

Zilker, D.P., Cook, G.W. and Hanratty, T.J. (1977), J. Fluid Mech., v. 82, pp. 29-51.

Zilker, D.P., Cook, G.W. and Hanratty, T.J. (1979), J. Fluid Mech., v. 90, pp. 257-271.

Table 1. Summary of the Experiments of Hanratty et al.

References	Measurements Made	Re	2a/λ	Flow Features Observed
Zilker et al. (1977)	wall pressure, wall shear,	3,000-32,000	0.0125 0.03125	linear shear stress response linear shear stress response
Zilker & Hanratty (1979)	mean velocity, turbulent velocity, flow visualizations		0.05 0.125 0.20	instantaneous flow reversal separated flow separated flow
Thorsness et al (1978)	wall shear, mean velocity	5,500-32,000	0.0114 0.0125	linear shear stress response linear shear stress response
Buckles et al (1984)	mean and fluctuating velocities and wall pressure	12,000	0.20	separated flow
Abrams (1984)	mean and fluctuating wall shear	5,970 - 122,500	0.014	linear shear stress response
Frederick (1986)	mean and fluctuating velocities	6,400 38,800	0.03125* 0.05	linear shear stress response nonlinear stress response
Kuzan (1986)	wall pressure, mean and fluctuating velocities, flow visualization	48,000 8,500 4,080	0.125 0.05 0.20*	instantaneous flow reversal instantaneous flow reversal separated flow

* present calculations were performed for these two cases

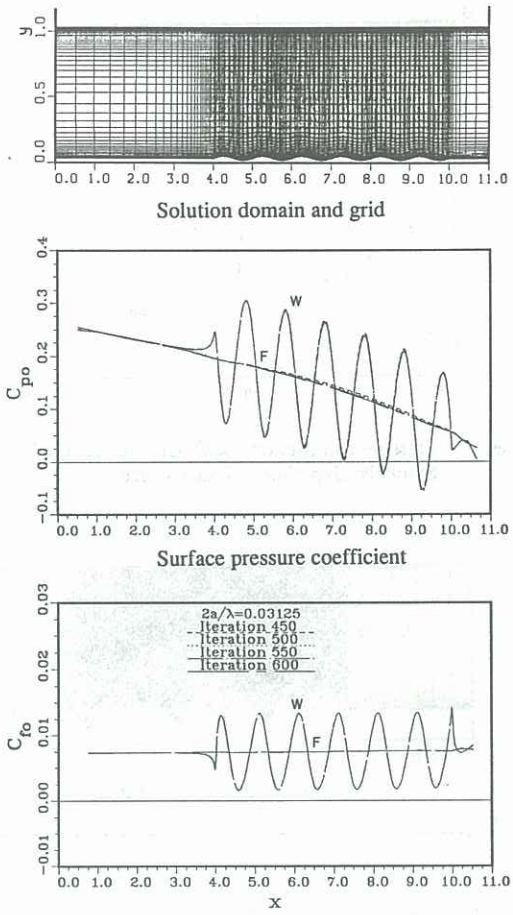

Figure 1. Channel with $2a/\lambda = 0.03125$.

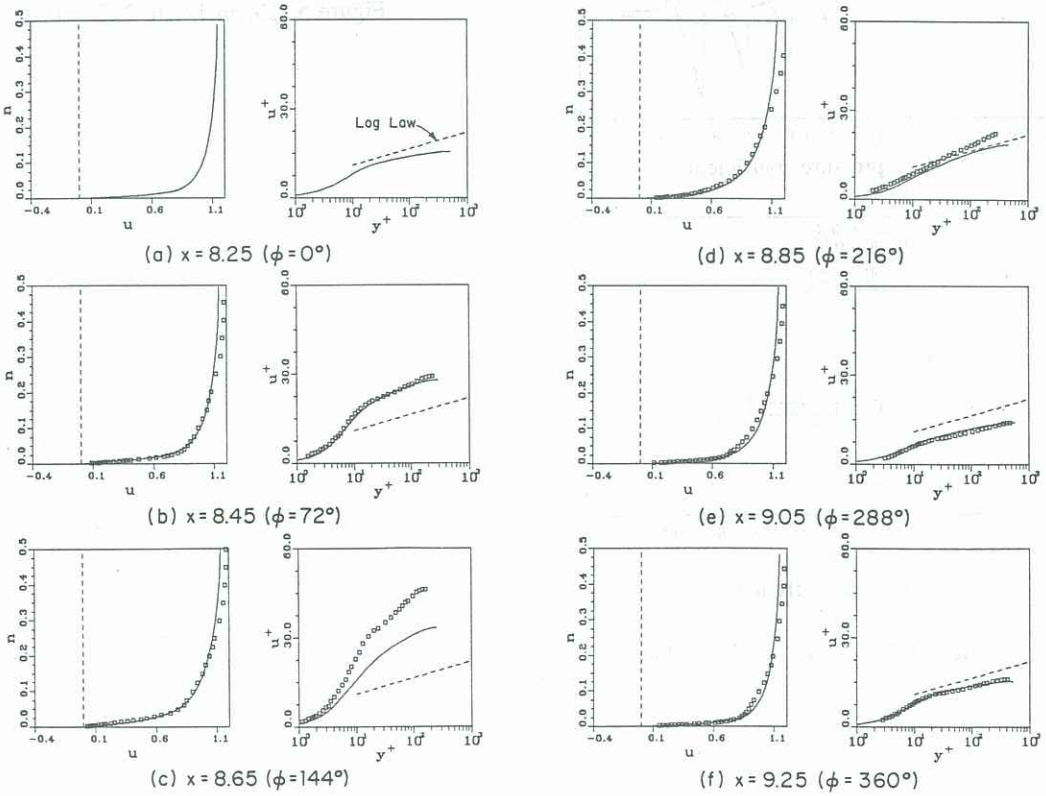

Figure 2. Velocity profiles for channel with $2a/\lambda = 0.03125$.
Symbols: Experiment; Lines: Calculation

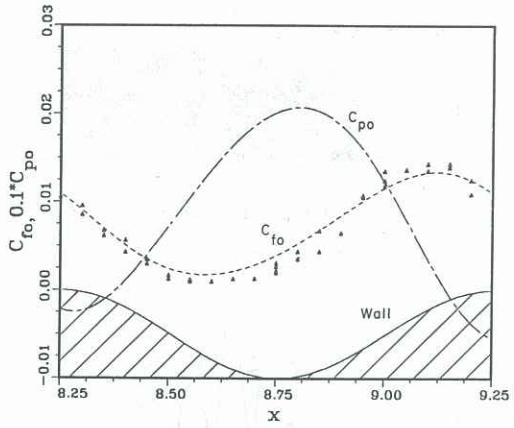

Figure 3. Pressure and friction coefficients for $2a/\lambda = 0.03125$.
Symbols: Experiment; Lines: Calculation

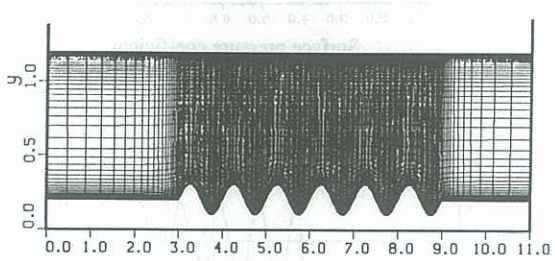

Solution domain and grid

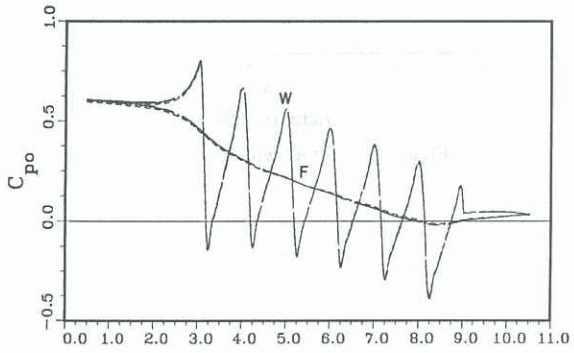

Surface pressure coefficient

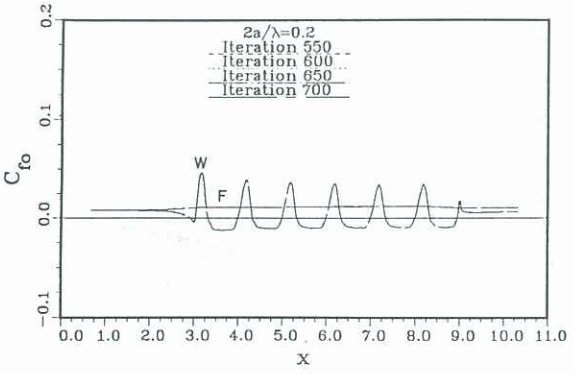

Friction coefficient

Figure 4. Channel with $2a/\lambda = 0.20$.

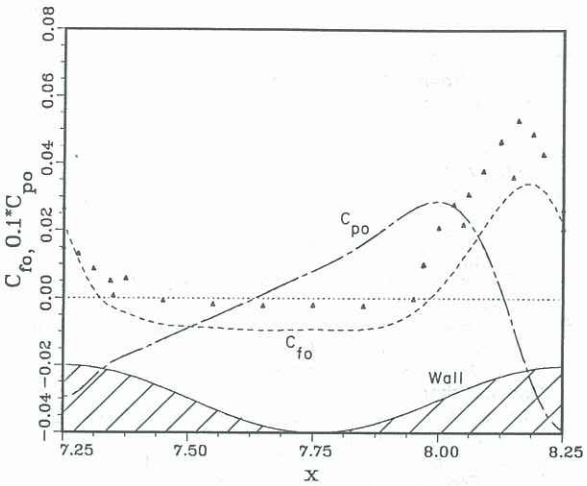

Pressure and friction coefficients;
data from Zilker and Kuzan

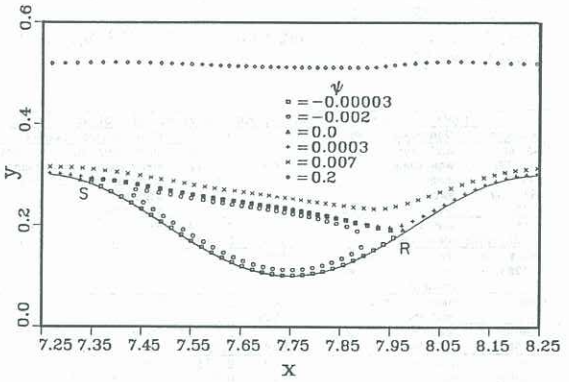

Calculated streamlines; S: separation, R: reattachment

Figure 5. Channel with $2a/\lambda = 0.20$.